Iron treatment inhibits Aβ42 deposition *in vivo* by modulating γ-secretase

and reducing Aβ42/Aβ40 ratio

〔鉄処理が γ セクレターゼを調節し A β 42/A β 40 比を下げることに

よって、*in vivo* での A β 42 の沈着を抑制する〕

Xuefeng Shen

Contents:

Abbreviations:

Aβ   Amyloid β-protein

APP   Amyloid precursor protein

BSA   Bovine serum albumin

CSF   Cerebral spinal fluid

CTF   C-terminal fragment

CX   Cortex

D-MEM   Dulbecco's modified eagle medium

DG   Dentate gyrus

EDTA   Ethylene diamine tetra acetic acid

GFAP   Glial fibrillary acidic protein

HP   Hippocampus

PBS   Phosphate buffered saline

TBST   Tris buffered saline with Tween20

WB   Western blotting

WT   Wild type

Abstract

Alzheimer's disease (AD) is characterized by the formation of extracellular amyloid plaques containing the amyloid β-protein (Aβ) within the parenchyma of the brain. Aβ42, which is 42 amino acids in length, is considered to be the key pathogenic factor in AD. Iron deposition is found abundantly in the amyloid plaques of AD patients; however, whether iron intake exacerbates amyloid deposition *in vivo* is unknown. Here, we treated AD model mice with iron-containing water and found that Aβ42 deposition in the brain was significantly inhibited, along with a decrease in iron deposition. Iron treatment did not change the overall levels of iron in the brain or serum. Interestingly, Aβ40 generation was significantly increased by iron treatment in amyloid precursor protein (APP)-overexpressing fibroblasts, whereas Aβ42 generation did not change, which led to a decreased Aβ42/Aβ40 ratio. We found that ferritin bound to presenilin 1 and that iron treatment increased this binding. Because Aβ40 can inhibit Aβ42 aggregation *in vitro*, and Aβ40 inhibits amyloid formation *in vivo*, our results suggest that iron can selectively enhance Aβ40 generation by modulating γ-secretase and inhibit amyloid deposition by reducing the Aβ42/Aβ40 ratio. Thus, iron may be used as a novel treatment for reducing the Aβ42/Aβ40 ratio and Aβ42 deposition in AD.

Introduction

Alzheimer's disease (AD) is a progressive, fatal neurodegenerative disease characterized clinically by progressive loss of memory and cognitive decline. The neuropathological hallmarks of AD are the accumulation of amyloid-β protein (Aβ) in extracellular plaques, neurofibrillary tangles that are composed of intracellular abnormally-phosphorylated tau, and neuronal loss (1). Aβ is generated from amyloid precursor protein (APP) through sequential cleavage by two proteases called β- and γ-secretases. Proteolytic processing of APP to generate Aβ is somewhat heterogeneous, resulting in production of Aβ peptides of different lengths, with the differences mainly at the carboxyl terminus of the peptide. The two most common isoforms of Aβ are 40 and 42 residues in length, depending on the site of γ-secretase cleavage (2). Although secreted Aβ40 is much more abundant than Aβ42, Aβ42 is considered the causative molecule for triggering the onset of AD because it is more prone to aggregation and is the major component in senile plaques. In contrast, Aβ40 can inhibit Aβ42 toxicity and accumulation of Aβ42 in the brain (3-5).

Iron accumulates in the brain of patients with several neurodegenerative diseases, such as AD and Parkinson's disease (6,7). Increased accumulation of iron in amyloid plaques and neurofibrillary tangles of the AD brain has been reported in human post-mortem studies (8). In AD model mice, the correlation between amyloid plaque morphology and iron biochemistry

provides evidence for the formation of an iron-amyloid complex (9). Several *in vitro* studies have demonstrated that iron promotes the aggregation, oligomerization, and toxicity of Aβ42 (10,11). In addition, the interaction between Aβ42 and metal ions, such as iron and copper may play a crucial role in the release of reactive oxygen species, which contribute to neurodegenerative damage (12,13). Free transitional iron is also toxic. This results largely from "Fenton chemistry", which allows the reversible transition from the ferrous (Fe^{2+}) to the ferric (Fe^{3+}) state to produce reactive oxygen species (14). However, the oxidative toxicity of the transitional metals can be inhibited by interaction with monomeric Aβ40 *in vitro* (15). In contrast, the same redox chemistry of iron can catalyze electron-transfer reactions, as iron serves as a prosthetic group for proteins involved in central cellular processes, including oxygen transport, mitochondrial respiration, DNA synthesis, cell growth, and differentiation (14). In the central nervous system, iron and iron-binding proteins play crucial roles in normal brain function, various processes of brain development, including myelin synthesis, neurotransmitter synthesis, and metabolism, and maintenance of the high metabolic and energetic requirements of neuronal tissues (7). Based on human post-mortem analyses, the total iron deposition in the brain is positively correlated with age, suggesting that brain iron metabolism may decrease with aging (7,16). A recent study showed that levels of ferritin in cerebrospinal fluid are negatively associated with cognitive performance in normal individuals and

those with mild cognitive impairment and AD, suggesting a link between ferritin or brain iron levels and AD progression (17).

In light of these previous studies, we hypothesized that excess iron in the brain maybe a causative factor for AD onset. Here, we examined whether iron treatment could increase amyloid deposition *in vivo*. Contrary to our expectation, Aβ42 deposition significantly decreased in the brain of iron-treated AD model mice compared with control mice. In addition, tau phosphorylation and the number of apoptotic neurons also decreased in iron-treated AD model mice. We also found that iron treatment increased Aβ40 generation and reduced the Aβ42/Aβ40 ratio in human APP (hAPP)-overexpressing cells. To clarify this γ-secretase-modulating mechanism of iron, we further showed that iron increased the binding of ferritin to presenilin 1 (PS1), the catalytic component of γ-secretase, suggesting that binding may modulate γ-secretase to generate more Aβ40.

Materials and Methods

1. Iron treatment of AD model mice and preparation of brain tissue

Mice expressing hAPP bearing the Swedish and Indian mutations (hAPPSwInd, J20) were purchased from The Jackson Laboratory (Bar Harbor, ME, USA). All mice were housed on a 12-hour light/dark schedule with ad libitum access to food and water. For iron treatment, hAPPSwInd mice were treated with 1.3% ferrous sulfate in their drinking water from 6 to 14 months of age. All animal procedures were conducted in accordance with and approved by the Iwate Medical University Committee for Animal Use. Mice were killed at 14 months of age by inhalation of CO_2 and were then perfused intracardially with cold PBS containing 5 U/ml heparin (Sigma, St. Louis, MO, USA). The left hemisphere of the brain was fixed in 4% buffered paraformaldehyde solution at 4 °C for immunohistochemical analysis. Brain regions (cortex, hippocampus) were dissected from the right hemisphere and used for Aβ enzyme-linked immunosobent assay (ELISA). Brain sections (30-μm-thick) of the left hemisphere were prepared using a freezing microtome (SM2000R, Leica, Wetzla, Germany).

2. Thioflavin-S staining and immunohistochemistry

Thioflavin-S staining was performed as previously described (18). Immunostaining for Aβ42 and phosphorylated tau was performed using a Vectastain ABC Kit (Vector Laboratories, Burlingame, CA, USA). Anti-human amyloid β (1-42) rabbit polyclonal IgG (1:100) (IBL, Takasaki,

Japan) and anti-phosphorylated tau protein mouse monoclonal antibodies (1:100) (AT100, Thermo Scientific, Carlsbad, CA, USA) were used. For immunofluorescent staining of apoptotic neurons, brain sections were first stained with anti-cleaved caspase-3 (D175) rabbit polyclonal antibody (1:200) (Cell Signaling, Danvers, MA, USA) and secondary goat anti-rabbit Alexa Fluor 568 antibody (1:200) (Thermo Scientific), and then stained with an anti-NeuN rabbit polyclonal Alexa Fluor 488 antibody (1:100) (Merck, Kenilworth, NJ, USA). Anti-ferritin light chain rabbit polyclonal antibody (1:100) (Abcam, Cambridge, MA, USA) and anti-PS1 mouse monoclonal antibody (1:100) (Merck) were used. Goat anti-mouse Alexa Fluor 488 and goat anti-rabbit Alexa Fluor 568 secondary antibodies (Thermo Scientific) were diluted at 1:200. The number of thioflavin-S-positive plaques, the Aβ42-immunopositive area, and the number of AT100-immunopositive cells were quantitated in four sections per mouse brain by an observer blinded to the mouse group. The Aβ42-immunopositive area was measured using Image J (NIH, Bethesda, MD, USA). Neuronal apoptosis in the cortex was quantitated by counting the number of NeuN-positive cells with or without active caspase-3 signal in three random microscopic fields (500 μm × 500 μm) in the region of the lateral parietal association cortex and secondary visual cortex mediolateral area. Brain sections were imaged with a fluorescence microscope (BZ-9000, Keyence, Osaka, Japan) or a confocal microscope (Olympus FV 1000, Olympus, Tokyo, Japan).

3. Brain iron deposition staining and determination of the iron level

For detection of iron deposition, brain sections were incubated for 15 h in 7% potassium ferrocyanide in 3% aqueous hydrochloric acid and subsequently incubated in 0.75 mg/ml 3,39-diaminobenzidine and 0.015 % H_2O_2 for 5–10 min (8). The number of iron depositions in the hippocampus was counted in at least four sections per mouse brain by an observer blinded to the mouse group. For determination of the total iron level, serum samples were analyzed based on an internal-standard method, and brain samples were analyzed based on a standard-free method. Briefly, the target area was bombarded with a 2.9-MeV proton beam from a small size cyclotron after passing through two sets of triplet quadrupole magnets and a graphite collimator (5 mm in diameter), and the emitted X-rays were simultaneously measured with two Si (Li) detectors. A 300-μm Mylar absorber, which has been used for the detection of elements heavier than potassium, was used for detector No. 1. The beam spot size, typical beam current, and measuring time were 6 mm in diameter, 60 nA, and 6 to 10 min, respectively. Quantitative concentrations of elements were obtained from the X-ray spectra using the computer programs SAPIX and KEI.

4. Aβ ELISA

Mouse cortices were homogenized in 10 volumes of lysis buffer containing 5.0 M guanidine/HCl in 50 mM Tris/HCl, pH 8.0, and then stored at −80 °C until analysis, as described previously (18). The brain homogenate was diluted 1:2000 for Aβ42 ELISA and 1:20 for Aβ40 ELISA

in the dilution buffer provided in the ELISA kit (Wako, Osaka, Japan). Mouse embryonic fibroblasts were prepared from E13.5 embryos of hAPPSwInd mice as described previously (18). Wild type mouse embryonic fibroblasts stably expressing wild-type hAPP695 were also used (19). Cells were treated with ferrous sulfate after plating in 10% fetal bovine serum-DMEM (Wako, Osaka, Japan), and Aβ levels in the culture medium were determined after 72 h with ELISA. All samples were measured in triplicate.

5. Immunoblotting

Cell lysate from hAPPSwInd fibroblasts was prepared in RIPA buffer 72 h after treatment with ferrous sulfate. Protein (30 μg per sample) was separated by SDS-PAGE on a 5–20% gel and blotted onto hybond nitrocellulose membranes (GE Healthcare, Pittsburgh, PA, USA). The membranes were incubated with primary antibodies overnight at 4 °C. Appropriate peroxidase-conjugated secondary antibodies were applied, and the bound proteins were visualized by SuperSignal Chemiluminescence (Thermo Scientific). Membranes were stripped and reprobed with anti-β-actin antibody to normalize the loading amounts.

For immunoprecipitation, 5 μg antibodies were added to 200 μg cell lysate to pull down the target protein. Anti-nicastrin antibody and anti-β-actin antibody were purchased from Sigma-Aldrich. PS1-CTF antibody was from Millipore. Anti-PEN-2 antibody and anti-ferritin antibody were purchased from Abcam. Anti-Aph-1 antibody was from

COVANCE.

6. Statistical analysis

All data are shown as the mean ± standard error of the mean (SEM). We compared group differences with one-way analysis of variance (ANOVA) followed by the post-hoc Bonferroni/Dunn test for two or more groups against a control group. All data were analyzed with GraphPad Prism 5 (GraphPad, La Jolla, CA, USA). P values < 0.05 were considered statistically significant.

Result:

1. Iron treatment reduced Aβ42 deposition in the brain.

To study whether extra iron affected brain amyloid deposition in AD model mice, we treated hAPPSwInd mice with ferrous sulfate containing water from 6 to 14 months of age. In hAPPSwInd mice, amyloid plaque formation starts at 6 months of age and is abundant at 14 months of age (20). Contrary to our expectation, although iron promotes the aggregation and oligomerization of Aβ *in vitro*, iron treatment did not increase the brain amyloid deposition *in vivo*. On the contrary, iron markedly reduced the Aβ42-immunopositive area in the hippocampus to 53% compared with control mice (Fig. 1A and B). Quantitation of Aβ with ELISA also revealed a significant decrease in the level of Aβ42 in the cortex of iron-treated mice, whereas the Aβ40 level did not show a significant decrease (Fig. 1C and D). The number of thioflavin-S-positive plaques did not show a significant decrease in the hippocampus or cortex of iron-treated mice (Fig. 1E and F). Because thioflavin-S predominantly stains condensed amyloid plaques and Aβ42 immunostaining can visualize thioflavin-S-negative diffuse plaques, this result suggests that iron treatment mainly reduced the deposition of Aβ42 diffuse plaques.
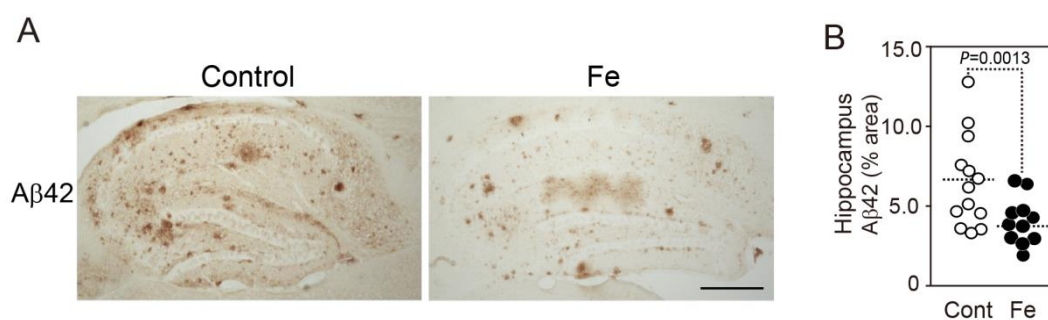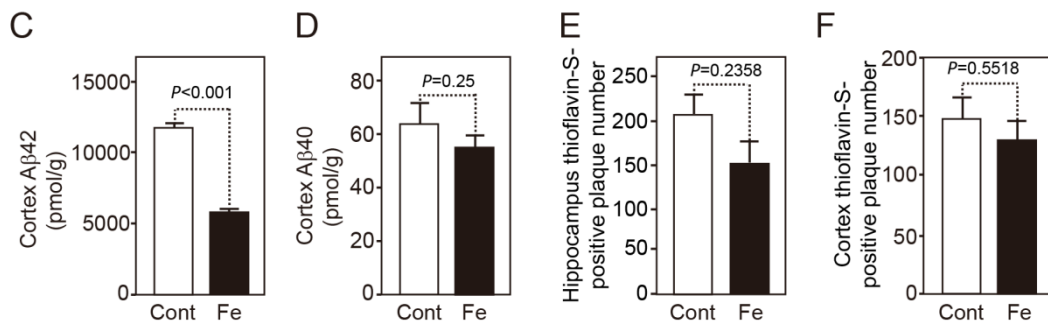
Fig. 1. A, Sagittal brain sections from 14-month-old hAPPSwInd mice treated with control water or ferrous sulfate water were stained with an antibody specific for Aβ42 to detect Aβ42 deposition. Representative images of hippocampi are shown. Scale bar = 500 μm. B, Determination of the immunopositive area demonstrated by anti-Aβ42 antibody in the hippocampus. n = 13 for the control group (Cont; open circles); n = 11 for the iron-treated group (Fe; filled circles). 2 to 4 brain sections were randomly selected from each mouse brain. Each dot on the figure is the average value of the quantitative results of several brain slices corresponding to the mouse. C and D, Aβ42 and Aβ40 levels determined by ELISA in the cortex of 14-month-old mice treated with control and ferrous sulfate-containing drinking water. n = 6 for the control group (Cont; open bars); n = 6 for the iron-treated group (Fe; filled bars).   E and F, Number of thioflavin-S-positive plaques in the hippocampus (E) and cortex (F) of the control and iron-treated mice. n = 13 for the control group (Cont; open bars); n = 11 for the iron-treated group (Fe; filled bars). 1 to 2 brain sections were randomly selected from each mouse brain. Data are the mean ± SEM; one-way ANOVA followed by the Bonferroni/Dunn test.

2. Iron deposition was decreased in the hippocampus of iron-treated mice.

Because iron accumulates in amyloid plaques in the brain of AD patients and AD model mice, we examined whether iron treatment affects iron deposition in the hippocampus of hAPPSwInd mice. Surprisingly, iron deposition significantly decreased by 39% in iron-treated mice compared with control mice (Fig. 2A and B). Because iron deposition is co-localized with amyloid plaques (8), this result suggests that iron deposition in the brain is dependent on amyloid plaque formation, but not the intake of iron. We further determined the total levels of iron in the serum and in the neocortex of iron-treated mice. The total level of iron in iron-treated mice did not differ from that of control mice, suggesting that iron can be maintained at a normal level both in the blood and in the brain with this iron treatment (Fig. 2C and D). Ferritin is an important intracellular iron binding protein, which is involved in the iron metabolism. When iron metabolism is activated, the level of ferritin increases. In order to confirm that iron treatment did activate iron metabolism, we conducted immunoblotting to detect ferritin level in the kidney of mice (Fig. 2E). As a result, iron treatment markedly increased ferritin level in kidney. It suggests that oral intake of iron activated iron metabolism of mice.
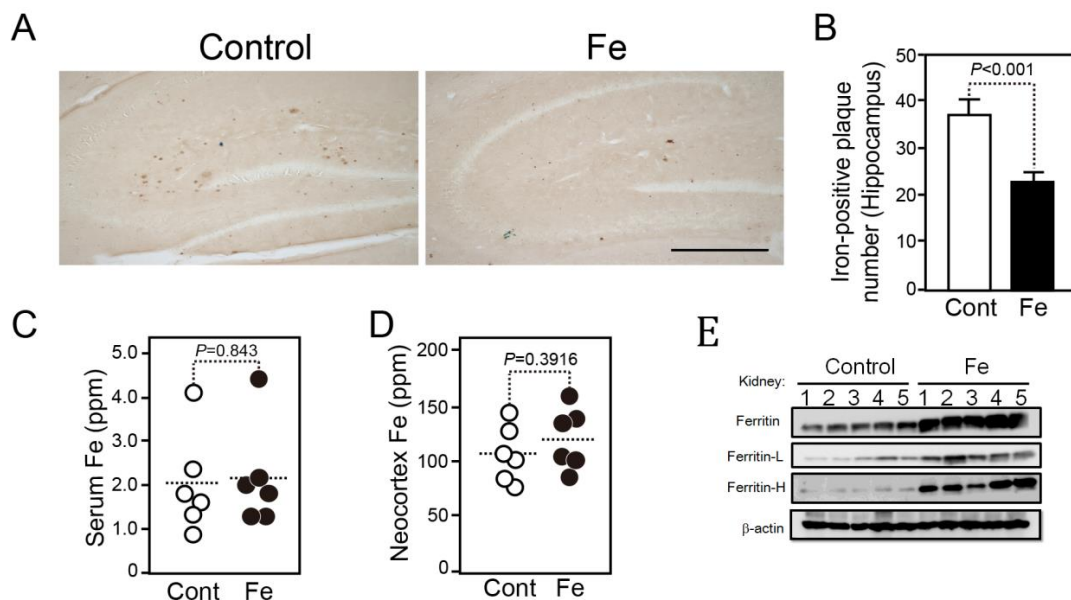
Fig. 2. A. Comparison of iron deposition in the hippocampus of control and ferrous sulfate water-treated 14-month-old hAPPSwInd mice. Representative images of hippocampus are shown. Scale bar = 500 μm. B. Number of iron-positive plaques in the hippocampus of 14-month-old hAPPSwInd mice with or without iron treatment. n = 13 for the control group (Cont; open bars); n = 11 for the iron-treated group (Fe; filled bars). 1 to 2 brain sections were randomly selected from each mouse. C and D, The iron concentration in the serum (C) and neocortex (D) from control and iron-treated mice was determined using a proton beam and an X-ray spectra technique. n = 6 for the control group (Cont; open circles); n = 6 for the iron-treated group (Fe; filled circles). Each dot on the figure is the average of the quantitative results of several brain slices of the mouse. E, The ferritin level in the kidney of mice was detected by immunoblotting; n = 5 for each group. Data are the mean ± SEM; one-way ANOVA followed by the Bonferroni/Dunn test.

3. Iron modulates γ-secretase and reduces the Aβ42/Aβ40 ratio.

To examine whether iron regulates Aβ generation, we treated mouse embryonic fibroblasts overexpressing wild-type hAPP (19) and embryonic fibroblasts from hAPPSwInd mice with ferrous sulfate and measured Aβ secretion in the culture medium. Treatment with 10 μM ferrous sulfate significantly increased Aβ40 generation 1.5-fold compared with untreated hAPP fibroblasts, whereas Aβ42 generation did not show a significant increase (Fig. 3A and B). The increase in Aβ40 resulted in a significant, 25.6 % decrease in the Aβ42/Aβ40 ratio (Fig. 3C). Similar results were also obtained from hAPPSwInd fibroblasts, in which the Aβ42/Aβ40 ratio was decreased 11.7 % by treatment with 5 μM ferrous sulfate ($P<0.05$). Because Aβ40 inhibits the aggregation, toxicity, and brain deposition of Aβ42 (3-5), this result suggests that iron may exhibit amyloid inhibitory and neuroprotective effects by reducing the Aβ42/Aβ40 ratio. To explore the mechanism underlying the effects of iron on regulation of γ-secretase, we further examined the levels of components of γ-secretase, including Aph-1, PS1, nicastrin and PEN-2. We found that iron-treatment did not change the cellular levels of Aph1, PS1 carboxyl terminal fragment (PS1-CTF), nicastrin, or PEN-2 (Fig. 3G). PS1-CTF is a part of active γ-secretase that is generated from endocleavage of PS1 (21). Ferritin is a cytosolic iron storage protein composed of a mixture of 24 subunits of ferritin light chain (ferritin-L) and ferritin heavy chain (ferritin-H) (22). Notably, ferritin levels were markedly and dose-dependently increased by iron treatment (Fig. 3D).

We next perform immunoprecipitation studies to examine whether the increase in ferritin is associated with the γ-secretase complex. Ferritin-L was associated with PS1-CTF and PEN-2, and the amount of PS1-CTF and PEN-2 bound to ferritin-L was increased by iron treatment (Fig. 3E). We also found a similar association between ferritin-H and PS1-CTF. However, different from ferritin-L, ferritin-H did not bind to PEN-2 (Fig. 3F). With immunostaining, we confirmed that the intracellular level of ferritin-L was significantly increased by iron treatment (Fig. 3H, left panels). The PS1 level did not change (Fig. 3H, middle panels), and the co-localization of ferritin-L and PS1 was increased in the iron-treated cells (Fig. 3H, right panels).
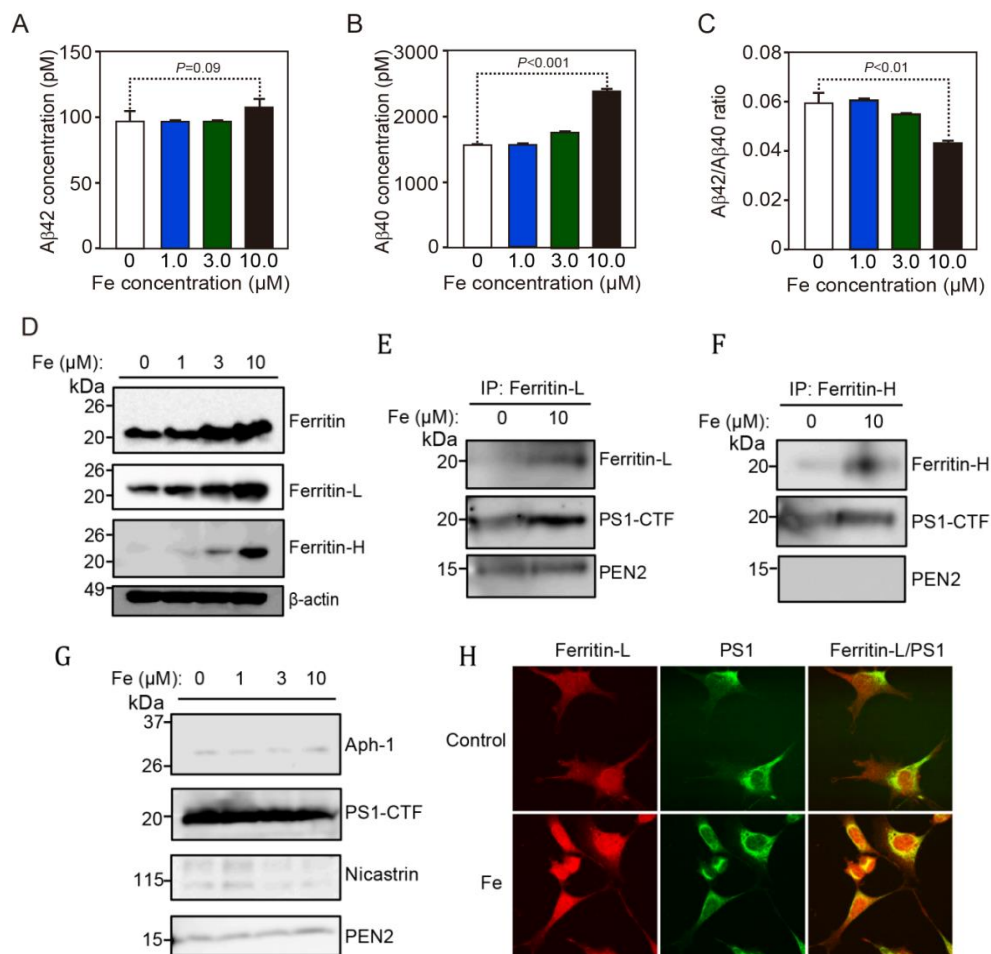
Fig. 3. A and B, Aβ42 and Aβ40 concentrations in the culture medium of hAPP695-overexpressing fibroblasts treated with ferrous sulfate. C, The Aβ42/Aβ40 ratio was reduced by iron treatment in a dose-dependent manner. D, Immunoblot analysis of total ferritin, ferritin-L, and ferritin-H in hAPP695-overexpressing fibroblasts treated with ferrous sulfate. E, Co-immunoprecipitation analysis shows the interaction between ferritin-L and PS1-CTF or PEN-2. F, Co-immunoprecipitation analysis shows the interaction between ferritin-H and PS1-CTF. G, Immunoblot analysis of Aph-1, PS1-CTF, nicastrin and PEN-2 in hAPP695-overexpressing fibroblasts treated with ferrous sulfate. H, hAPP695-overexpressing fibroblasts treated with or without ferrous sulfate were immunostained with anti-ferritin-L and anti-PS1 antibodies. Confocal microscopy revealed that ferritin-L was increased by iron treatment and that the co-localization of ferritin-L and PS1 was also increased by iron treatment. n = 6. Data are the mean ± SEM; one-way ANOVA followed by the Bonferroni/Dunn test.

4. Iron treatment reduced phosphorylated tau protein and apoptotic neurons *in vivo*.

Phosphorylated and aggregated tau in neurons is another hallmark of AD and is thought to be secondary to amyloid pathology (23). We also examined phosphorylated tau in the brain of iron-treated hAPPSwInd mice using the AT100 antibody, which recognizes phosphorylated threonine 212 and serine 214 of tau protein. The number of AT100-positive neurons was reduced in the cortex by iron treatment compared with the control group (Fig. 4A and B). In addition, the number of apoptotic neurons in the cortex identified by anti-NeuN and anti-active caspase-3 antibodies showed a significant decrease in the iron-treated mice (Fig. 4C and D). These results suggest that the inhibition of Aβ42 deposition by iron treatment can reduce the phosphorylation of tau protein and neuronal apoptosis.
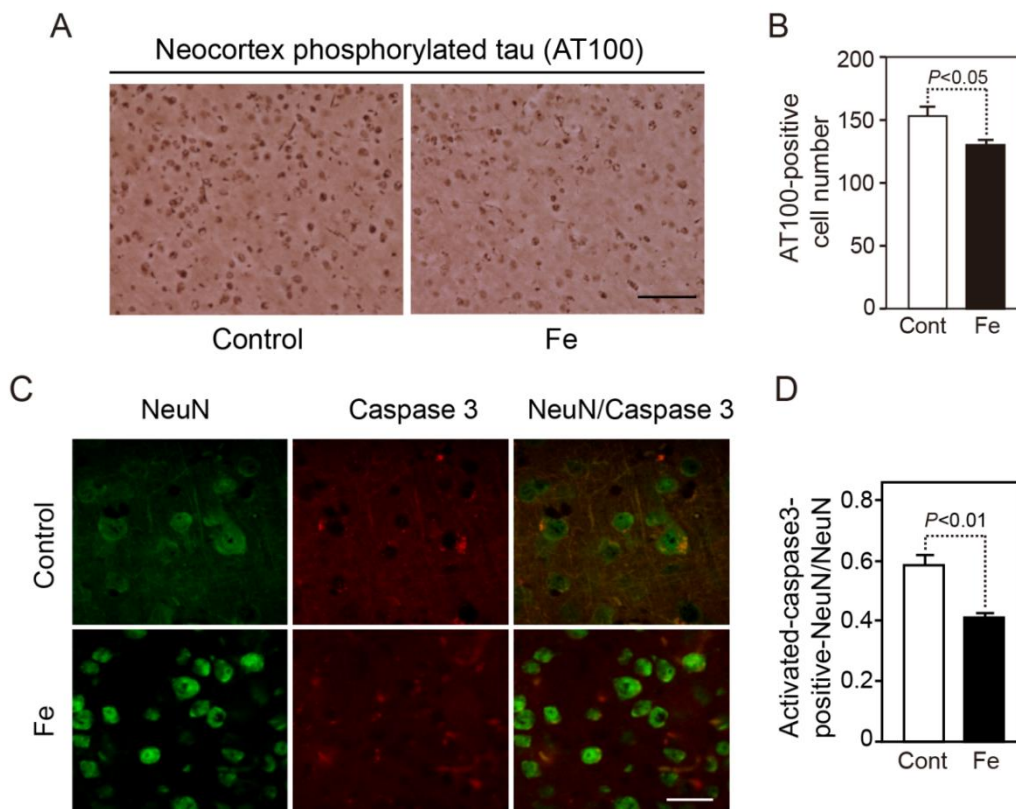
Fig. 4. A, Brain sections from 14-month-old hAPPSwInd mice were stained using anti-phosphorylated tau antibody (AT100). Representative images of the neocortex are shown. B, The number of AT100-positive neurons was lower in the neocortex of iron-treated mice than control mice. C and D, Brain sections from 14-month-old hAPPSwInd mice were stained using anti-NeuN and anti-active caspase-3 antibodies. Representative images of the neocortex are shown. Confocal microscopy revealed that the number of caspase-3-positive apoptotic neurons was lower in the iron-treated group than the control group. n = 13 for control group (Cont; open bars); n=11 for iron-treated group (Fe; filled bars). 1 to 2 brain sections were randomly selected from each mouse. Data are the mean ± SEM; one-way ANOVA followed by the Bonferroni/Dunn test. Scale bars: A, 100 μm; C, 20 μm.

Discussion

Iron plays a fundamental role in the development of the central nervous system and is an essential metal that is commonly used in the treatment of iron deficiency anemia. A lack of iron in organisms leads to many diseases, such as iron deficiency anemia, abnormalities dopamine metabolism, and spiral ganglion degeneration (24). Brain iron dyshomeostasis is associated with aging, which is accompanied by a progressive decline in cognitive processes and is also associated with several neurodegenerative disorders such as Alzheimer's, Parkinson's, and Huntington's diseases (7, 14, 22). Some *in vitro* studies have revealed that iron can promote the aggregation, oligomerization, and toxicity of Aβ42 (10, 11). However, little is known about whether iron treatment enhances brain Aβ deposition, or about whether intake of excess iron induces iron deposition *in vivo*. Here, unexpectedly, we found that iron treatment reduced Aβ42 deposition and iron deposition in the brain of AD model mice. Furthermore, we demonstrated that iron treatment modulates γ-secretase as indicated by increased Aβ40 generation, but not increased Aβ42 generation, thereby resulting in a decreased Aβ42/Aβ40 ratio. Then how can iron treatment modulate γ-secretase activity?

Ferritin is an important intracellular iron binding protein, which is involved in the iron metabolism. When iron metabolism is activated, the level of ferritin increases. We showed that cellular ferritin was significantly increased by iron treatment (Fig. 2E, Fig. 3D) and the level of PS1-CTF

bound to ferritin-L and ferritin-H was also increased by iron treatment (Fig. 3E and F), implying that the involvement of ferritin as a γ-secretase modulator. Although the mount of iron in the body did not change under the effect of homeostasis (Fig. 2C and D), an increase in iron intake might lead to increase in iron in the body and CNS for a moment, resulting in the significant induction of ferritin expression and the activation of iron metabolism. Even though our experiments only based on the results from a peripheral tissue (kidney) (Fig.2E) and *in vitro* system (fibroblast cells) (Fig. 3D), it is thought that Fe-dependent ferritin up-regulation occurs in various organs of the body because ferritin genes are expressed in all animal cells (32).

In our AD mouse model, the longer and more toxic form of Aβ, Aβ42, is the major component of amyloid plaques, whereas the shorter and less toxic form of Aβ, Aβ40, comprises a very small portion of amyloid plaques (20). Aβ42 aggregation and deposition in the brain is the central event in both familial and sporadic AD (2). In the present study, brain Aβ42 deposition was inhibited by iron treatment, whereas iron treatment did not decrease Aβ42 generation *in vitro*, but rather showed a tendency to increase Aβ42 generation (Fig. 3). The levels of the Aβ degrading enzyme, neprilysin, and angiotensin-convertin enzyme (ACE), which converts Aβ42 to Aβ40, did not change in the brain of iron-treated mice compared with control mice. These findings suggest that iron inhibits Aβ42 deposition not by inhibiting Aβ42 generation, or by enhancing Aβ42 degradation/conversion.

Interestingly, the Aβ42/Aβ40 ratio in cell culture medium was markedly reduced by iron treatment and was a result of a significant increase in the Aβ40 level (Fig. 3). Because Aβ40 appears to be protective, the Aβ42/Aβ40 ratio is more important than the absolute amount of Aβ42 (25). Familial AD mutations in PS1 appear to cause AD through a loss of function of γ-secretase, which leads to decreased Aβ40 generation and an increased Aβ42/Aβ40 ratio (26, 27). For the first time, we reported that iron treatment can reduce the Aβ42/Aβ40 ratio by modulating γ-secretase and increasing Aβ40 generation. Our results suggest that modulating γ-secretase to increase Aβ40 is a novel strategy to inhibit Aβ42 aggregation and deposition in the brain.

A high concentration of iron is present in insoluble amyloid plaques in patients with AD, and brain iron increases with aging (14, 22). In AD, whether excess Aβ42 captures iron to form amyloid plaques or whether excess iron induces Aβ42 deposition is not clear. Here, we showed that excess iron intake reduced not only Aβ42 deposition but also iron deposition in vivo and that iron treatment increased Aβ40 generation *in vitro*. Our results suggest that excess iron does not induce the formation of iron-rich amyloid plaques and that if Aβ42 deposition is inhibited, iron deposition will consequently decrease. Thus, Aβ42 aggregation, but not excess iron, may be the first event in the formation of iron-rich amyloid plaques. Previous studies showed that copper can promote the neurotoxic redox activity of Aβ and induce oxidative cross-linking of the peptide into

stable oligomers. Small molecules that interfere with Aβ-metal interactions rapidly improve cognition in AD model mice and in a small group of patients with AD (28, 29). Interestingly, iron can also abrogate copper-mediated neurotoxicity by inhibiting the generation of free radicals (30). In our study, apoptotic neurons were significantly decreased in the brain of iron-treated hAPPSwInd mice, suggesting that iron has neuroprotective effects by inhibiting Aβ42 aggregation or inhibiting the generation of copper-mediated free radicals.

To reduce the levels of toxic Aβ42 or the Aβ42/Aβ40 ratio, many γ-secretase inhibitors or modulators have been designed and tested in clinical trials, but none have succeeded (2, 31). For the first time, we found that iron reduced the Aβ42/Aβ40 ratio not by inhibiting Aβ42 generation, but by enhancing Aβ40 generation. Iron treatment significantly increased the intracellular ferritin level, and the binding between ferritin and the catalytic component of the γ-secretase complex, PS1, also increased with iron treatment, suggesting that ferritin can modulate the activity of γ-secretase. Iron treatment is commonly and widely used and is safe for treatment of iron deficiency anemia. Our present studies provide a simple way and a new insight for using iron to modulate γ-secretase and reduce the Aβ42/Aβ40 ratio to possibly prevent AD.

Acknowledgements:

Reference:

1. Scheltens, P. *et al.* Alzheimer's disease. *Lancet* **388**, 505-517, doi:10.1016/S0140-6736(15)01124-1 (2016).
2. Selkoe, D. J. & Hardy, J. The amyloid hypothesis of Alzheimer's disease at 25 years. *EMBO molecular medicine* **8**, 595-608, doi:10.15252/emmm.201606210 (2016).
3. Zou, K. *et al.* Amyloid beta-protein (Abeta)1-40 protects neurons from damage induced by Abeta1-42 in culture and in rat brain. *Journal of neurochemistry* **87**, 609-619, doi:2018 [pii] (2003).
4. Kim, J. *et al.* Abeta40 inhibits amyloid deposition in vivo. *The Journal of neuroscience : the official journal of the Society for Neuroscience* **27**, 627-633, doi:27/3/627 [pii]10.1523/JNEUROSCI.4849-06.2007 (2007).
5. Kuperstein, I. *et al.* Neurotoxicity of Alzheimer's disease Abeta peptides is induced by small changes in the Abeta42 to Abeta40 ratio. *The EMBO journal* **29**, 3408-3420, doi:10.1038/emboj.2010.211 (2010).
6. Zecca, L., Youdim, M. B., Riederer, P., Connor, J. R. & Crichton, R. R. Iron, brain ageing and neurodegenerative disorders. *Nature reviews. Neuroscience* **5**, 863-873, doi:10.1038/nrn1537 (2004).
7. Ward, R. J., Zucca, F. A., Duyn, J. H., Crichton, R. R. & Zecca, L. The role of iron in brain ageing and neurodegenerative disorders. *The Lancet. Neurology* **13**, 1045-1060, doi:10.1016/S1474-4422(14)70117-6 (2014).
8. Smith, M. A., Harris, P. L., Sayre, L. M. & Perry, G. Iron accumulation in Alzheimer disease is a source of redox-generated free radicals. *Proceedings of the National Academy of Sciences of the United States of America* **94**, 9866-9868 (1997).
9. Telling, N. D. *et al.* Iron Biochemistry is Correlated with Amyloid Plaque Morphology in an Established Mouse Model of Alzheimer's Disease. *Cell chemical biology* **24**, 1205-1215 e1203, doi:10.1016/j.chembiol.2017.07.014 (2017).
10. Huang, X. *et al.* Trace metal contamination initiates the apparent auto-aggregation, amyloidosis, and oligomerization of Alzheimer's Abeta peptides. *Journal of biological inorganic chemistry : JBIC : a publication of the Society of Biological Inorganic Chemistry* **9**, 954-960, doi:10.1007/s00775-004-0602-8 (2004).

11. Liu, B. *et al.* Iron promotes the toxicity of amyloid beta peptide by impeding its ordered aggregation. *The Journal of biological chemistry* **286**, 4248-4256, doi:10.1074/jbc.M110.158980 (2011).

12. Huang, X. *et al.* The A beta peptide of Alzheimer's disease directly produces hydrogen peroxide through metal ion reduction. *Biochemistry* **38**, 7609-7616, doi:10.1021/bi990438f (1999).

13. Jomova, K., Vondrakova, D., Lawson, M. & Valko, M. Metals, oxidative stress and neurodegenerative disorders. *Molecular and cellular biochemistry* **345**, 91-104, doi:10.1007/s11010-010-0563-x (2010).

14. Ashraf, A., Clark, M. & So, P. W. The Aging of Iron Man. *Frontiers in aging neuroscience* **10**, 65, doi:10.3389/fnagi.2018.00065 (2018).

15. Zou, K., Gong, J. S., Yanagisawa, K. & Michikawa, M. A novel function of monomeric amyloid beta-protein serving as an antioxidant molecule against metal-induced oxidative damage. *The Journal of neuroscience : the official journal of the Society for Neuroscience* **22**, 4833-4841 (2002).

16. Zecca, L. *et al.* The role of iron and copper molecules in the neuronal vulnerability of locus coeruleus and substantia nigra during aging. *Proceedings of the National Academy of Sciences of the United States of America* **101**, 9843-9848, doi:10.1073/pnas.0403495101 (2004).

17. Ayton, S., Faux, N. G., Bush, A. I. & Alzheimer's Disease Neuroimaging, I. Ferritin levels in the cerebrospinal fluid predict Alzheimer's disease outcomes and are regulated by APOE. *Nature communications* **6**, 6760, doi:10.1038/ncomms7760 (2015).

18. Liu, J. *et al.* Angiotensin type 1a receptor deficiency decreases amyloid beta-protein generation and ameliorates brain amyloid pathology. *Scientific reports* **5**, 12059, doi:10.1038/srep12059 (2015).

19. Komano, H. *et al.* A new functional screening system for identification of regulators for the generation of amyloid beta-protein. *The Journal of biological chemistry* **277**, 39627-39633, doi:10.1074/jbc.M205255200 (2002).

20. Mucke, L. *et al.* High-level neuronal expression of abeta 1-42 in wild-type human amyloid protein precursor transgenic mice: synaptotoxicity without plaque formation. *The Journal of neuroscience : the official journal of the Society for Neuroscience* **20**, 4050-4058 (2000).

21. De Strooper, B., Iwatsubo, T. & Wolfe, M. S. Presenilins and gamma-secretase: structure, function, and role in Alzheimer Disease. *Cold Spring Harbor perspectives in medicine* **2**, a006304, doi:10.1101/cshperspect.a006304 (2012).

22. Belaidi, A. A. & Bush, A. I. Iron neurochemistry in Alzheimer's disease and Parkinson's disease: targets for therapeutics. *Journal of neurochemistry* **139 Suppl 1**, 179-197, doi:10.1111/jnc.13425 (2016).

23. Mandelkow, E. M. & Mandelkow, E. Biochemistry and cell biology of tau protein in neurofibrillary degeneration. *Cold Spring Harbor perspectives in medicine* **2**, a006247, doi:10.1101/cshperspect.a006247 (2012).

24. Camaschella, C. Iron-deficiency anemia. *The New England journal of medicine* **372**, 1832-1843, doi:10.1056/NEJMra1401038 (2015).

25. Tanzi, R. E. & Bertram, L. Twenty years of the Alzheimer's disease amyloid hypothesis: a genetic perspective. *Cell* **120**, 545-555, doi:10.1016/j.cell.2005.02.008

(2005).

26. Shen, J. & Kelleher, R. J., 3rd. The presenilin hypothesis of Alzheimer's disease: evidence for a loss-of-function pathogenic mechanism. *Proceedings of the National Academy of Sciences of the United States of America* **104**, 403-409, doi:10.1073/pnas.0608332104 (2007).

27. Quintero-Monzon, O. *et al.* Dissociation between the processivity and total activity of gamma-secretase: implications for the mechanism of Alzheimer's disease-causing presenilin mutations. *Biochemistry* **50**, 9023-9035, doi:10.1021/bi2007146 (2011).

28. Adlard, P. A. *et al.* Rapid restoration of cognition in Alzheimer's transgenic mice with 8-hydroxy quinoline analogs is associated with decreased interstitial Abeta. *Neuron* **59**, 43-55, doi:10.1016/j.neuron.2008.06.018 (2008).

29. Faux, N. G. *et al.* PBT2 rapidly improves cognition in Alzheimer's Disease: additional phase II analyses. *Journal of Alzheimer's disease : JAD* **20**, 509-516, doi:10.3233/JAD-2010-1390 (2010).

30. White, A. R. *et al.* Iron inhibits neurotoxicity induced by trace copper and biological reductants. *Journal of biological inorganic chemistry : JBIC : a publication of the Society of Biological Inorganic Chemistry* **9**, 269-280, doi:10.1007/s00775-004-0521-8 (2004).

31. Sacks, C. A., Avorn, J. & Kesselheim, A. S. The Failure of Solanezumab - How the FDA Saved Taxpayers Billions. *The New England journal of medicine* **376**, 1706-1708, doi:10.1056/NEJMp1701047 (2017).

32. Paolo, A. *et al.* Ferritin, cellular iron storage and regulation. *International Union of Biochemistry and Molecular Biology: IUBMB: a journal of Biochemistry and Molecular Biology* **69** 6 414-422 doi.org/10.1002/iub.1621(2017).